OL Organic Letters

pubs.acs.org/OrgLett

Letter

Brominated B_1-Polycyclic Aromatic Hydrocarbons for the Synthesis of Deep-Red to Near-Infrared Delayed Fluorescence Emitters

Kang Yuan, Abhishek Kumar Gupta, Changfeng Si, Marina Uzelac, Eli Zysman-Colman,* and Michael James Ingleson*

Cite This: https://doi.org/10.1021/acs.orglett.3c02167

Read Online

ACCESS | Metrics & More | Article Recommendations | Supporting Information

ABSTRACT: Bromo-functionalized B_1-polycyclic aromatic hydrocarbons (PAHs) with LUMOs of less than −3.0 eV were synthesized and used in cross-couplings to form donor−acceptor materials. These materials spanned a range of S_1 energies, with a number showing thermally activated delayed fluorescence and significant emission in the near-infrared region of the spectrum. These B_1-PAHs represent a useful family of acceptors that can be readily synthesized and functionalized.

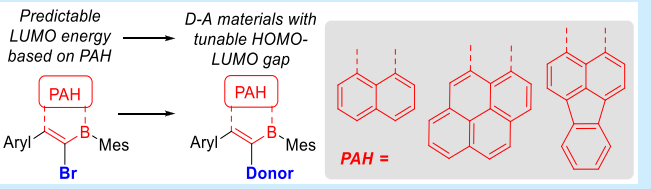

The incorporation of boron into polycyclic aromatic hydrocarbons (PAHs) has attracted significant attention as a method for modulating key optoelectronic properties.[1] Due to the electron deficiency of the boron center in C_3B units, PAHs containing these moieties (termed B-PAHs) often have stabilized LUMOs (relative to all carbon PAH analogues).[2] This is exemplified by comparing anthracene (LUMO ≈ −2.4 eV)[3] to 9,10-diboranthracene [DBA (Figure 1a)], with the latter having a much lower energy LUMO (approximately −3 eV).[4] Recent breakthroughs have enabled access to B-doped PAHs with deep LUMOs (defined herein as less than −3.0 eV).[5] This has led to their use in organic electronics applications that require strong acceptors.[6] However, accessing deep LUMO B-PAHs generally requires the incorporation of multiple boron centers into the PAH core,[5,7] which increases the synthetic complexity. Furthermore, the use of deep LUMO B-PAHs as strong acceptor units in donor−acceptor (D−A) materials remains underexplored despite the ubiquity of these materials in applications, including in deep-red- and near-infrared-emitting OLEDs.[8] This paucity is in part due to the shortage of readily accessible deep LUMO B-PAHs that contain a group amenable to functionalization, particularly through cross-coupling reactions.[9]

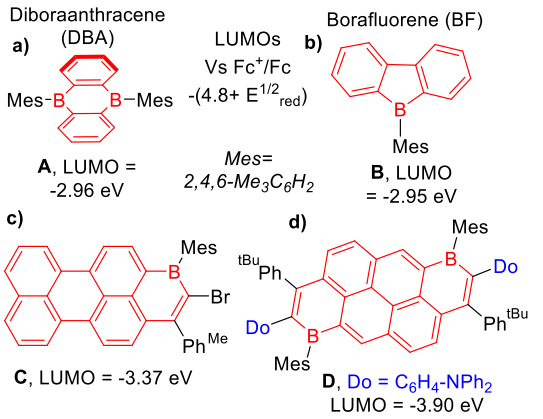

Figure 1. Select previous work on low-LUMO B-PAHs (top) and previous work accessing and using deep LUMO B-PAHs (bottom).

An analysis of reported low-energy LUMO B-PAH-based D−A emissive materials reveals that most are based on DBA or borafluorene (BF) cores (Figure 1b).[10] While notable D−A materials have been reported using DBA and BF, including red thermally activated delayed fluorescence (TADF) emitters,[11] the LUMO of these two B-doped PAHs is approximately −3.0 eV (in the absence of electron-withdrawing groups).[12] This LUMO energy makes it challenging to access D−A materials with emission maxima shifted far into the deep-red and near-infrared (near-IR) region of the spectrum. Furthermore, when DBA and BF are used in D−A materials, the donor unit is often installed as part of the exocyclic group on boron.[10,11] An alternative approach that we reported recently involves the formation of brominated B-PAHs via the treatment of alkyne-substituted PAHs with BBr_3.[13] This one-pot procedure produced bench-stable deep LUMO compounds, such as **C** (Figure 1c). This method was applied to the synthesis of several brominated B-PAHs, with the vinyl bromide unit being

Received: July 4, 2023

attractive for use in cross-coupling reactions. However, in our initial work, only one D−A material was synthesized, and while this compound [**D** (Figure 1d)] had a small HOMO−LUMO gap, it could be synthesized in only poor overall yield (12% from the alkyne) and it did not display delayed fluorescence. The latter was attributed from calculations to an overly large singlet−triplet excited state gap, ΔE_{ST}. The low yield of compounds such as **D** complicated attempts to access other D−A materials based on these B_2-PAHs, precluding structure−property relationship studies.

Herein, we report that B_1-PAHs made through this methodology are useful for accessing families of D−A materials with tunable HOMO−LUMO gaps and S_1 energies. The deep S_1 energies of these materials indicate that this family of acceptors can help meet the call set out in a recent review on near-IR emitters that stated, "the development of new functionalized acceptor units with simple structures is still imperative".[8]

Our previous work used alkynyl-naphthalene, -pyrene, and -perylene derivatives, which were transformed into B_1-PAHs using BBr_3.[13b] At the outset of this study, three B_1-PAHs were analyzed by cyclic voltammetry (CV), which revealed that the LUMO energy of the B_1-PAH correlated to the LUMO energy of the PAH core (red, Figure 2). In each case, calculations

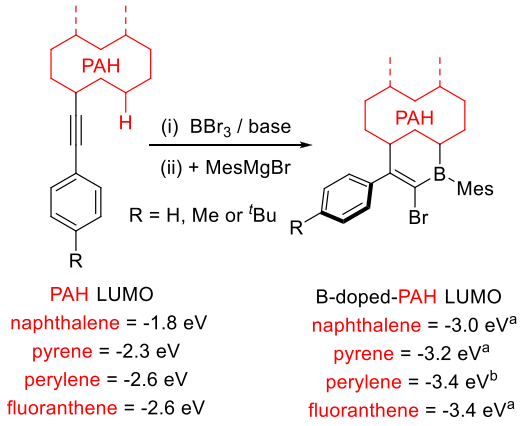

Figure 2. Effect of varying the PAH on the LUMO energy of B_1-PAH. $E_{LUMO} = -E_{1/2}^{red} = 4.8$ eV. [a]This work and [b]ref 13b.

indicated that the LUMO is localized across the PAH and the boracycle. If this correlation is general, then a PAH with a LUMO energy comparable to that of perylene should give a B_1-PAH with a deep LUMO. Indeed, a B_1-PAH derived from fluoranthene was synthesized and found to possess a LUMO energy comparable to that of the perylene analogue (Figure 2).

Three B_1-PAHs with different LUMO energies were studied further. To assess the effect bromide has on the LUMO energy, a phenyl was installed to form compounds **1**−**3** (Figure 3) via Negishi cross-coupling reactions. This had a minimal effect on the LUMO energy, with **1**−**3** being harder to reduce than the bromo derivatives by only 0.05−0.1 V (Figures S43−S50 and Table S1). In each case, the calculated LUMO remained localized over the boracycle and PAH units (Figure S40). This indicated that low-HOMO−LUMO gap/deep S_1 energy materials would be accessible by installing donor units at this position. Therefore, a number of D−A materials were modeled to guide synthetic studies. Triphenylamine (TPA) was selected on the basis of calculations (Figure S38), which revealed that **4**−**6** (Figure 3) span a range of S_1 energies, with all having an

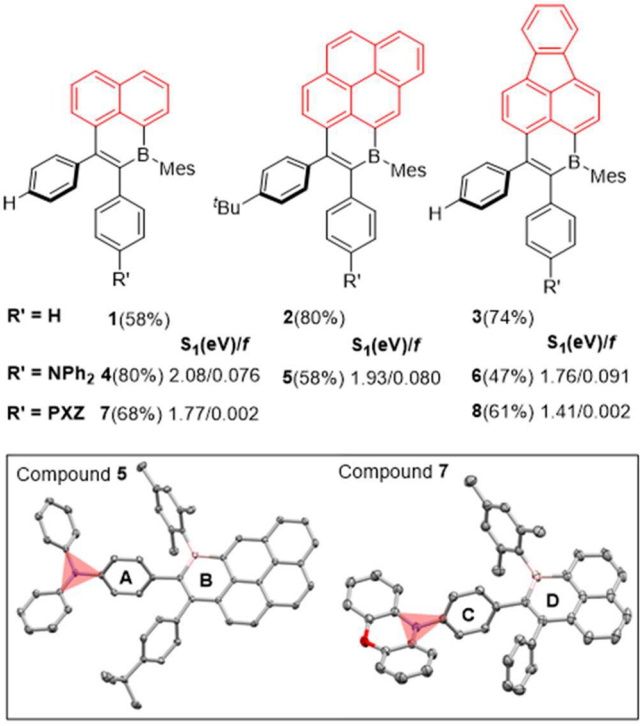

Figure 3. Compounds **1**−**8**. Yields (in parentheses) are for the Negishi coupling, with calculated S_1 energy and f values for **4**−**8** (top). Solid state structures of **5** and **7** (bottom), where the ellipsoids are drawn at the 50% probability level with hydrogens omitted.

appreciable oscillator strength (f) for the S_0−S_1 transition. Furthermore, small (≤0.25 eV) ΔE_{ST} values were calculated, and thus, TADF behavior was expected. The calculated small ΔE_{ST} is consistent with both S_1 and T_1 states for **4**−**6** possessing significant charge transfer (CT) character (Figures S39 and S41). Calculations were also performed on **7** (Figure 3), which contains a *p*-phenoxazine-phenyl (PXZ-Ph) donor. While **7** had a calculated S_1 energy similar to that of **6**, the f value associated with the CT-dominated S_0−S_1 transition was negligible, attributed to the strongly twisted conformation. Analysis of **4**−**6** revealed that the HOMO is distributed on both the donor and the boracycle (Figures S38 and S41); thus, there is appreciable spatial overlap with the LUMO, essential for an appreciable f. However, for **7**, the HOMO is localized on the PXZ unit, dramatically reducing the extent of spatial overlap with the LUMO (Figure S42). Thus, while the calculated ΔE_{ST} was very small for **7**, it was expected to be a very weak near-IR emitter. Finally, a PXZ-Ph fluoranthene derivative, **8**, was calculated. Analogous to **7**, **8** has a CT-dominated S_0−S_1 transition with a very low f. Nevertheless, the calculated small HOMO−LUMO gap of **8** indicates it may have potential in non-emissive applications.[14]

Compounds **4**−**8** were synthesized using the same Negishi cross-coupling conditions in respectable overall yields (35−45% from the alkyne). The twisted D−A nature of **4**−**8** suggested by the calculations was supported by single-crystal X-ray diffraction studies of **5** and **7** (Figure 3, bottom). This revealed that the B_1-PAH and the phenyl-N ring are twisted, with the angle between the planes of rings A and B in **5** being 58.1° and that between rings C and D in **7** being 61.5°. Both the boron and nitrogen centers are effectively planar (Σ_{C-N-C} values of 357.5° and 355.4° for **5** and **7**, respectively). Another informative metric is the angle between the C_3N plane (red

https://doi.org/10.1021/acs.orglett.3c02167
Org. Lett. XXXX, XXX, XXX−XXX

Table 1. Optoelectronic Properties of 3−8

	$E_{1/2}^{red}$ (V)[a]	$E_{1/2}^{ox}$ (V)[a]	LUMO^{exp} (eV)[b]	optical gap (eV)[c]	λ_{PL}^{Tol} (nm)[d]	Φ_{PL}^{Tol} (%)[e]	λ_{PL}^{CBP} (nm)[f]	Φ_{PL} (%)[g]	S_1/T_1 (eV)[h]	τ (ns)[f]	τ (μs)[e]
3	−1.46	–	−3.34	2.09	501	5 (5)	495	25.4 (25.2)	2.82/2.43	5.7	–
4	−1.84	0.50	−2.96	2.23	630	42 (36)	623	39.0 (38.5)	2.26/2.23	80	2.4
5	−1.69	0.50	−3.11	1.94	700	3 (3)	682	6.2 (5.8)	2.10/2.08	2.8	1.1
6	−1.48	0.50	−3.32	1.87	745	4 (4)	738	2.8 (2.1)	1.95/1.89	2.1	1.0
7	−1.79	0.34	−3.01	2.41	660	9 (5)	614	31.7 (23.6)	2.29/2.12	52	1.9
8	−1.45	0.34	−3.35	2.06	780	4 (4)	673	4.2 (4.0)	2.09/2.01	–	–

[a]At 298 K in THF with 0.1 M [^{n}Bu$_4$N]PF$_6$ (vs Fc$^+$/Fc). [b]$E_{LUMO} = -E_{1/2}^{red} - 4.8$ eV. [c]From the onset of the absorption in toluene. [d]At 298 K, in degassed toluene at 1×10^{-5} M. [e]At 298 K, in degassed toluene with values in parentheses under aerated conditions. [f]In spin-coated 5 wt % doped films in CBP at 298 K. [g]Spin-coated films of 5 wt % emitters doped in CBP under N_2 with the values in parentheses in air. [h]Obtained from the onset of the steady state photoluminescence and phosphorescence spectra (1−9 ms) at 77 K of 5 wt % films in CBP.

triangle in Figure 3) and ring A/C, which is 53.1° and 78.9° for **5** and **7**, respectively. This suggests less effective orbital mixing between the NAr_2 unit and the bridging phenyl for PXZ in **7** relative to NPh_2 in **5**, consistent with the lower *f* for the S_0-S_1 HOMO−LUMO-dominated transition for the PXZ derivatives.

The frontier orbital energies for **4**−**8** were probed by CV, with all displaying a reversible first reduction wave (Figures S51−S57). The LUMO energy is deepest for the fluoranthene B_1-PAH derivatives (Table 1), with the LUMO energy effectively identical across the Ph-, TPA-, and PXZ-Ph-substituted derivatives (e.g., **3** vs **6** vs **8**). This is consistent with the LUMO being localized on B_1-PAH in each case. Notably, the LUMOs are deeper for the B_1-PAHs containing pyrene and fluoranthene (e.g., **5** and **6**) than those of DBA and BF (with B-Mes substituents). The donor dominates the first oxidation process for **4**−**8**, with the PXZ-Ph derivatives having a ∼0.15 eV destabilized HOMO energy relative to the TPA congeners.

With regard to the solution state photophysical properties, weak broad absorption bands are observed in **4**−**6** (Figure 4a), which are assigned to CT transitions based on calculations (Figure S39). There is the expected shift to lower energies of the CT band across these three compounds, which is aligned with the increasing acceptor strength of the B_1-PAH. Compared to **4**−**6**, there are no obvious CT absorption bands for **7** and **8** consistent with the negligible *f* calculated for the S_0-S_1 transitions in these two compounds. All D−A compounds exhibit unstructured and broad photoluminescence (PL) spectra in toluene (Figure 4a), indicative of an excited state with strong CT character. For the TPA series, the emission bands are red-shifted with maxima (λ_{PL}) at 630, 700, and 745 nm for **4**−**6**, respectively, consistent with the progressively stabilized computed S_1 energies. As expected, the use of the stronger donor PXZ in **7** and **8** produces a more red-shifted emission (λ_{PL} at 660 and 780 nm) in toluene compared to TPA analogues **4** and **6**, respectively. The PL spectra of each of the D−A compounds exhibit strong positive solvatochromism (Figure S58) and become broader with an increase in solvent polarity, consistent with the CT nature of the emissive excited state.

Next, the photoluminescence behavior of **4**−**8** was measured as thin films in PMMA (Figure S60). **4**−**6** exhibited λ_{PL} values similar to those in toluene; however, **7** and **8** showed blue-shifted emission compared to those in toluene (λ_{PL} at 580 and 670 nm, respectively). This is tentatively assigned to PXZ adopting a different conformation in PMMA, which has been previously observed.[15] We then investigated the photophysical

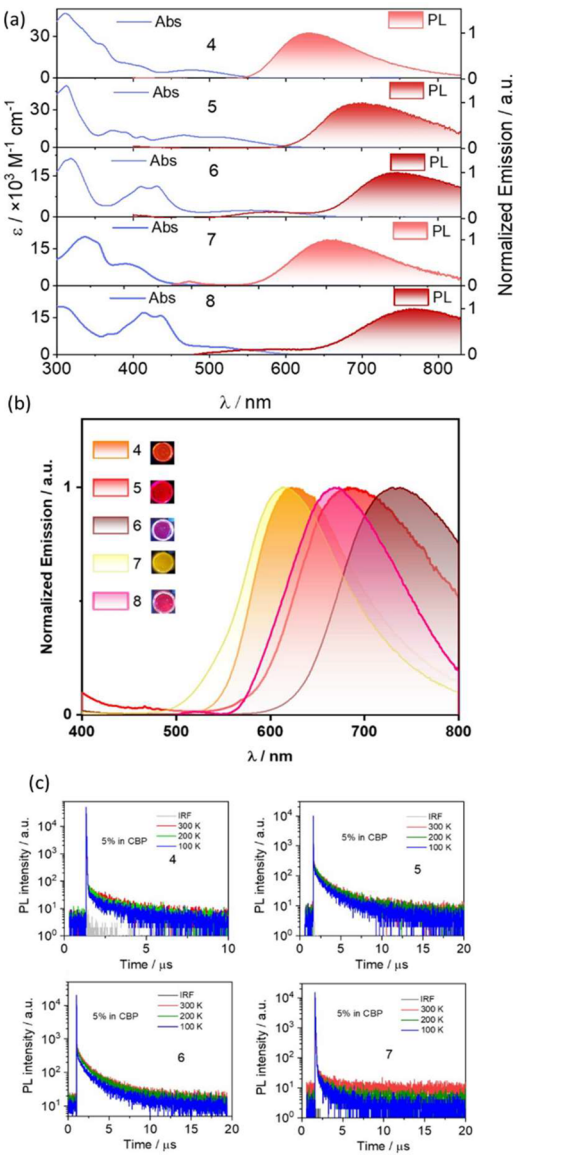

Figure 4. (a) UV−vis absorption and PL spectra of **4**−**8** in toluene (λ_{exc} = 330 nm). (b) Emission spectra of 5 wt % doped films of **4**−**8** in CBP (λ_{exc} = 330 nm). (c) Time-correlated single-photon counting plots for **4**−**7** (λ_{exc} = 375 nm).

behavior of the emitters in 4,4′-bis(*N*-carbazolyl)-1,1′-biphenyl (CBP) that has a high triplet energy (2.55 eV).[16] Compounds **4**−**6** emit at 623, 682, and 738 nm (Figure 4b), respectively, with Φ_{PL} values of 39.0%, 6.2%, and 2.8%, respectively (Table

https://doi.org/10.1021/acs.orglett.3c02167
Org. Lett. XXXX, XXX, XXX−XXX

1). The time-resolved PL of **4**–**6** reveals (Figure 4c) biexponential decay kinetics consisting of a nanosecond prompt component and a microsecond delayed component (Table 1). The delayed emission tended to increase with temperature, which is consistent with TADF for these three compounds. With regard to the PXZ derivatives, the λ_{PL} again is significantly blue-shifted compared to the emission of **7** and **8** in toluene (Table 1); this is tentatively assigned to PXZ adopting a different conformation in CBP films.[15] The TADF nature of the emission from **7** was confirmed by the temperature-dependent nature of the delayed emission (Figure 4c). Delayed emission was not detected for **8** in CBP. Finally, the S_1/T_1 energies were probed at 77 K for **4**–**8** (Figure S66), with the S_1/T_1 states being close in energy, consistent with the observed TADF (Table 1).

In summary, this work introduces a series of bench-stable bromo-functionalized B_1-PAHs that have LUMOs ranging between −3.0 and −3.4 eV. They can be used to form D−A materials all under the same Negishi coupling conditions in moderate yields. A number of the D−A materials displayed TADF with significant emission in the near-IR region of the spectrum. This work demonstrates the promise of using these readily accessible boron-doped arenes as strong acceptors to produce NIR-emitting TADF compounds.

■ ASSOCIATED CONTENT

Data Availability Statement

The data underlying this study are available in the published article and its Supporting Information.

Supporting Information

The Supporting Information is available free of charge at https://pubs.acs.org/doi/10.1021/acs.orglett.3c02167.

Full experimental details, NMR spectra for all new compounds, crystal structures, and plots of optoelectronic data (PDF)
Cartesian coordinates (XYZ)
Cartesian coordinates (XYZ)
Cartesian coordinates (XYZ)
Cartesian coordinates (XYZ)
Cartesian coordinates (XYZ)
Cartesian coordinates (XYZ)
Cartesian coordinates (XYZ)
Cartesian coordinates (XYZ)

Accession Codes

CCDC 2265859−2265860 contain the supplementary crystallographic data for this paper. These data can be obtained free of charge via www.ccdc.cam.ac.uk/data_request/cif, or by emailing data_request@ccdc.cam.ac.uk, or by contacting The Cambridge Crystallographic Data Centre, 12 Union Road, Cambridge CB2 1EZ, UK; fax: +44 1223 336033.

■ AUTHOR INFORMATION

Corresponding Authors

Michael James Ingleson − *EaStCHEM School of Chemistry, The University of Edinburgh, Edinburgh EH9 3FJ, U.K.*; orcid.org/0000-0001-9975-8302; Email: michael.ingleson@ed.ac.uk

Eli Zysman-Colman − *Organic Semiconductor Centre and EaStCHEM School of Chemistry, University of St Andrews, St Andrews KY16 9ST, U.K.*; orcid.org/0000-0001-7183-6022; Email: eli.zysman-colman@st-andrews.ac.uk

Authors

Kang Yuan − *EaStCHEM School of Chemistry, The University of Edinburgh, Edinburgh EH9 3FJ, U.K.*

Abhishek Kumar Gupta − *Organic Semiconductor Centre and EaStCHEM School of Chemistry, University of St Andrews, St Andrews KY16 9ST, U.K.*; orcid.org/0000-0002-0203-6256

Changfeng Si − *Organic Semiconductor Centre and EaStCHEM School of Chemistry, University of St Andrews, St Andrews KY16 9ST, U.K.*

Marina Uzelac − *EaStCHEM School of Chemistry, The University of Edinburgh, Edinburgh EH9 3FJ, U.K.*

Complete contact information is available at: https://pubs.acs.org/10.1021/acs.orglett.3c02167

Notes

The authors declare no competing financial interest.

■ ACKNOWLEDGMENTS

This project has received funding from the Leverhulme Trust (Grant RPG-2022-032) and the European Research Council (ERC) under the European Union's Horizon 2020 research and innovation program (Grant Agreement 769599). C.S. thanks the China Scholarship Council (201806890001), and M.I. and E.Z.-C. thank the EPSRC Programme Grant "Boron: Beyond the Reagent" (EP/W007517) for support.

■ REFERENCES

(1) For representative recent reviews, see: (a) Wang, R.; Lee, C.-S.; Lu, Z. Recent development of three-coordinated boron-doped aromatics for optoelectronic applications. *J. Organomet. Chem.* **2023**, *984*, 122564. (b) Shi, J.; Ran, Z.; Peng, F.; Chen, M.; Li, L.; Ji, L.; Huang, W. High-performance three-coordinated organoboron emitters for organic light-emitting diodes. *J. Mater. Chem. C* **2022**, *10*, 9165−9191. (c) Mellerup, S. K.; Wang, S. Boron-doped molecules for optoelectronics. *Trends Chem.* **2019**, *1*, 77−89. (d) von Grotthuss, E.; John, A.; Kaese, T.; Wagner, M. Doping polycyclic aromatics with boron for superior performance in materials science and catalysis. *Asian J. Org. Chem.* **2018**, *7*, 37−53. (e) Ji, L.; Griesbeck, S.; Marder, T. B. Recent developments in and perspectives on three-coordinate boron materials: a bright future. *Chem. Sci.* **2017**, *8*, 846−863.

(2) For recent reviews on this topic, see: (a) Yin, X.; Liu, J.; Jäkle, F. Electron-Deficient Conjugated Materials via p-π^* Conjugation with Boron: Extending Monomers to Oligomers, Macrocycles, and Polymers. *Chem. - Eur. J.* **2021**, *27*, 2973−2986. (b) Hirai, M.; Tanaka, N.; Sakai, N.; Yamaguchi, S. Structurally Constrained Boron-, Nitrogen-, Silicon-, and Phosphorus-Centered Polycyclic π-Conjugated Systems. *Chem. Rev.* **2019**, *119*, 8291−8331.

(3) Energies of the PAHs used in this work are taken from: Davis, A. P.; Fry, A. J. Experimental and Computed Absolute Redox Potentials of Polycyclic Aromatic Hydrocarbons are Highly Linearly Correlated Over a Wide Range of Structures and Potentials. *J. Phys. Chem. A* **2010**, *114*, 12299−12304.

(4) Hoffend, C.; Diefenbach, M.; Januszewski, E.; Bolte, M.; Lerner, H.-W.; Holthausen, M. C.; Wagner, M. Effects of boron doping on the structural and optoelectronic properties of 9,10-diarylanthracenes. *Dalton Trans.* **2013**, *42*, 13826−13837.

(5) For select recent examples of deep LUMO B-PAHs, see: (a) Guo, J.; Zhang, K.; Wang, Y.; Wei, H.; Xiao, W.; Yang, K.; Zeng, Z. Fully-fused boron-doped olympicenes: modular synthesis, tunable optoelectronic properties, and one-electron reduction. *Chem. Sci.* **2023**, *14*, 4158−4165. (b) Mützel, C.; Farrell, J. M.; Shoyama, K.; Würthner, F. 12b,24b-Diborahexabenzo[a,c,fg,l,n,qr]pentacene: A Low-LUMO Boron-Doped Polycyclic Aromatic Hydrocarbon. *Angew. Chem., Int. Ed.* **2022**, *61*, No. e202115746. (c) Liao, G.;

Chen, X.; Qiao, Y.; Liu, K.; Wang, N.; Chen, P.; Yin, X. Highly Electron-Deficient Dicyanomethylene-Functionalized Triarylboranes with Low-Lying LUMO and Strong Lewis Acidity. *Org. Lett.* **2021**, *23*, 5836−5841. (d) Xia, Y.; Zhang, M.; Ren, S.; Song, J.; Ye, J.; Humphrey, M. G.; Zheng, C.; Wang, K.; Zhang, X. 6,12-Dihydro-6,12-diboradibenzo[def,mno]chrysene: A Doubly Boron-Doped Polycyclic Aromatic Hydrocarbon for Organic Light Emitting Diodes by a One-Pot Synthesis. *Org. Lett.* **2020**, *22*, 7942−7946.

(6) For a recent review on this topic, see: Guo, Y.; Chen, C.; Wang, X.-Y. Recent Advances in Boron-Containing Acenes: Synthesis, Properties, and Optoelectronic Applications. *Chin. J. Chem.* **2023**, *41*, 1355−1373.

(7) For select examples, see: (a) Farrell, J. M.; Mutzel, C.; Bialas, D.; Rudolf, M.; Menekse, K.; Krause, A. M.; Stolte, M.; Würthner, F. Tunable low-LUMO boron-doped polycyclic aromatic hydrocarbons by general one-pot C-H borylations. *J. Am. Chem. Soc.* **2019**, *141*, 9096−9104. (b) Radtke, J.; Schickedanz, K.; Bamberg, M.; Menduti, L.; Schollmeyer, D.; Bolte, M.; Lerner, H. W.; Wagner, M. *Chem. Sci.* **2019**, *10*, 9017−9027. (c) Ito, M.; Sakai, M.; Ando, N.; Yamaguchi, S. Electron-Deficient Heteroacenes that Contain Two Boron Atoms: Near-Infrared Fluorescence Based on a Push-Pull Effect. *Angew. Chem. Int. Ed* **2021**, *60*, 21853−21859. (d) Kahan, R. J.; Crossley, D. L.; Cid, J.; Radcliffe, J. E.; Woodward, A. W.; Fasano, V.; Endres, S.; Whitehead, G. F. S.; Ingleson, M. J. Generation of a series of B_n fused oligo-naphthalenes (n = 1 to 3) from a B1-polycyclic aromatic hydrocarbon. *Chem. Commun.* **2018**, *54*, 9490−9493.

(8) Xiao, Y.; Wang, H.; Xie, Z.; Shen, M.; Huang, R.; Miao, Y.; Liu, G.; Yu, T.; Huang, W. NIR TADF emitters and OLEDs: challenges, progress, and perspectives. *Chem. Sci.* **2022**, *13*, 8906−8923.

(9) For an example of a halogenated deep-LUMO B_2-PAH useful in cross-coupling reactions see: Brend'amour, S.; Gilmer, J.; Bolte, M.; Lerner, H.-W.; Wagner, M. C-Halogenated 9,10-Diboraanthracenes: How the Halogen Load and Distribution Influences Key Optoelectronic Properties. *Chem. - Eur. J.* **2018**, *24*, 16910−16918.

(10) For select examples, see: (a) Chen, X.; Meng, G.; Liao, G.; Rauch, F.; He, J.; Friedrich, A.; Marder, T. B.; Wang, N.; Chen, P.; Wang, S.; Yin, X. Highly Emissive 9-Borafluorene Derivatives: Synthesis, Photophysical Properties and Device Fabrication. *Chem. - Eur. J.* **2021**, *27*, 6274−6282. (b) Li, Y.; Chen, X.; Zhang, W.; Zhang, J.; Xu, L.; Qiao, Y.; Liu, K.; Wang, N.; Chen, P.; Yin, X. Substituent Modulation for Highly Bright 9-Borafluorene Derivatives with Carbazole Pendant. *Org. Lett.* **2021**, *23*, 7236−7241. (c) Reus, C.; Weidlich, S.; Bolte, M.; Lerner, H.-W.; Wagner, M. C-Functionalized, Air- and Water-Stable 9,10-Dihydro-9,10-diboraanthracenes: Efficient Blue to Red Emitting Luminophores. *J. Am. Chem. Soc.* **2013**, *135*, 12892−12907.

(11) (a) Kumar, A.; Shin, H. Y.; Lee, T.; Jung, J.; Jung, B. J.; Lee, M. H. Doubly Boron-Doped TADF Emitters Decorated with ortho-Donor Groups for Highly Efficient Green to Red OLEDs. *Chem. - Eur. J.* **2020**, *26*, 16793−16801. (b) Hsieh, C.-M.; Wu, T.-L.; Jayakumar, J.; Wang, Y.-C.; Ko, C.-L.; Hung, W.-Y.; Lin, T.-C.; Wu, H.-H.; Lin, K.-H.; Lin, C.-H.; Hsieh, S.; Cheng, C.-H. Diboron-Based Delayed Fluorescent Emitters with Orange-to-Red Emission and Superior Organic Light-Emitting Diode Efficiency. *ACS Appl. Mater. Interfaces* **2020**, *12*, 23199−23206.

(12) Note, the use of "fluoro-mesityl" (and derivatives) as an exocyclic group on boron in place of mesityl, or the addition of other electron-withdrawing groups, enables access to deeper LUMO B_n-PAHs (including examples with LUMOs of less than −3.0 eV). For example, see: (a) Zhang, Z.; Edkins, R. M.; Haehnel, M.; Wehner, M.; Eichhorn, A.; Mailänder, L.; Meier, M.; Brand, J.; Brede, F.; Müller-Buschbaum, K.; Braunschweig, H.; Marder, T. B. Taming the Beast: Fluoromesityl Groups Induce a Dramatic Stability Enhancement in Boroles. *Chem. Sci.* **2015**, *6*, 5922−5927. (b) Jin, T.; Bolte, M.; Lerner, H.-W.; Wagner, M. Nucleophilic aromatic substitution approach to phosphanyl-substituted diboraanthracenes: biphilic compounds with tunable electron affinities. *Org. Chem. Front.* **2022**, *9*, 5611−5616.

(13) (a) Kahan, R. J.; Crossley, D. L.; Cid, J.; Radcliffe, J. E.; Ingleson, M. J. Synthesis, Characterization, and Functionalization of 1-Boraphenalenes. *Angew. Chem. Int. Ed* **2018**, *57*, 8084−8088. (b) Yuan, K.; Kahan, R. J.; Si, C.; Williams, A.; Kirschner, S.; Uzelac, M.; Zysman-Colman, E.; Ingleson, M. J. The synthesis of brominated-boron-doped PAHs by alkyne 1,1-bromoboration: mechanistic and functionalisation studies. *Chem. Sci.* **2020**, *11*, 3258−3267.

(14) For a select example, see: Cheng, P.; Yang, Y. Narrowing the Band Gap: The Key to High-Performance Organic Photovoltaics. *Acc. Chem. Res.* **2020**, *53*, 1218−1228.

(15) Cheng, Z.; Liang, J.; Li, Z.; Yang, T.; Lin, C.; Mu, X.; Wang, Y. Photoluminescent manipulation of phenoxazine based molecules via regulating conformational isomerization, and the corresponding electroluminescent properties. *J. Mater. Chem. C* **2019**, *7*, 14255−14263.

(16) Xu, T.; Yi, R.; Zhu, C.; Lin, M. Simple-Structured OLEDs Incorporating Undoped Phosphorescent Emitters Within Non-Exciplex Forming Interfaces: Towards Ultraslow Efficiency Roll-Off and Low Driving Voltage for Indoor R/G/B Illumination. *Front. Chem.* **2021**, *8*, 630687.

https://doi.org/10.1021/acs.orglett.3c02167
Org. Lett. XXXX, XXX, XXX−XXX